Exploring the Structural, charge density and molecular docking analysis of Coumarins [2H-1-benzopyran-2-one] molecule via Quantum chemical calculations

P. Srinivasan[a*], A. David Stephen[b*] and G. Rajalakshmi[c]

[a]Department of Physics, Chikkaiah Naicker College, Erode, Tamilnadu, India.
[b]Department of Physics, Sri Shakthi Institute of Engineering and Technology, Coimbatore, Tamilnadu, India
[c]Department of Physics, Sri Vijay Vidyalaya college of arts and Science, Dharmapuri, Tamilnadu, India

The Coumarin [2H-1-benzopyran-2-one] is used for antibacterial, antioxidant and anticancer agents. The docking analysis was carried out from Coumarin [2H-1-benzopyran-2-one] with cytochromeP450. The optimized geometry and charge density analysis of 2H-1-benzopyran-2-one molecule were obtained from the DFT methods with 6-311G** basis set. Further, a molecular docking analysis has been carried out to understand the conformational change and electrostatic properties of 2H-1-benzopyran-2-one in the active site of cytochromeP450 Receptor. MEP (Molecular Electrostatic Potential) is very useful investigation of the charge distributions of Coumarin [2H-1-benzopyran-2-one] molecule.

Keywords: DFT, Docking studies, Charge density, Dipole moment and ESP

Introduction

Antioxidants in biological systems have multiple functions which include protection from oxidative damage and in the major signalling pathways of cells [1,2]. The major action of antioxidant in cell is to prevent damage caused by the action of reactive oxygen species (ROS), such as superoxide, hydroxyl, peroxide and nitric acid radicals are generated in living organisms during excessive metabolism [3]. ROS cause extensive oxidative damage to cells leading to age related degenerative disease, cancer, and a wide range of other human disease [4,5]. Several synthetic antioxidants, such as butylated hydroxyl anisole (BHA), butylated hydroxytoluene (BHT), tertbutylhydroquinone (TBHQ) as well as propyl gallate are currently in use [6]. However, their uses have been limited for the fact that they may be responsible for liver damage and carcinogenesis [7]. For this reason, this problem has been overcome by new synthetic or natural compounds.

Coumarins and their derivatives have been found to exhibit a variety of biological and pharmacological activities and have raised considerable interest because of their potential beneficial effects on human health [8]. The Coumarin 2H-1-benzopyran-2-one, (Figure. 1) obtained from various part of plant like fruits, nuts and seeds are known to have better dietary value and more than 1300 coumarins have been identified from natural sources. They have been reported to possess among others: antibiotic, antibacterials, antitumor, antiviral agents, anticoagulants, against psoriasis, antioxidant, anticancer, anti-inflammatory, analgesic and diuretic properties [9]. Biological activity of coumarins has becoming an appealing point of studies owing to its different effects to diseases and less damage to normal cells [8]. In the recent years, the coumarin chalcone fibrates can down-regulate the phospholipids (PL), total cholesterol (TC), and triglycerides (TG), and regulate the levels of VLDL, LDL and HDL. Apart from the medicinal applications coumarins are also used as sweetener, fixative of perfumes, enhancer of natural oils such as lavender, a food additive in combination with vanillin, a flavour/odour stabilizer in tobacco, an odour masker in paints and rubber. Owning to the widespread applications, docking, charge density and biological activity evaluation of coumarins molecule has been a subject of intense investigations.

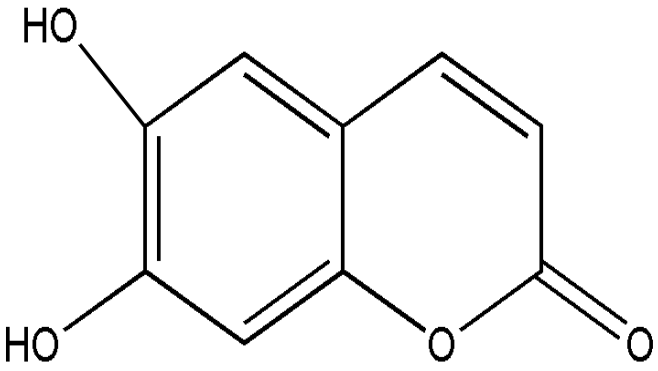

Figure.1 Crystal Structure of Coumarins (2H-1-benzopyran-2-one) molecule

*Corresponding Author: **sriniscience@gmail.com**

(Received May 5, 2017; Accepted September 4, 2017)

2. Computational Details

The receptor cytochrome P450 with pdb code 1TQN [10] was obtained from Brookhaven Protein Data bank. The ligand was drawn using Chemdraw software. The molecular docking analysis has been performed using AUTODOCK program [11]. After docking analysis 10 lowest energy conformers were obtained. Among them, the lowest energy conformer was used for docking study. The PyMOL [12] software was used to view the intermolecular interactions that exist between the receptor and the ligand. An *Ab initio* [13] and DFT single point energy calculations were performed for the molecule lifted from the active site using B3LYP [14, 15] and 6-311G** basis set with the Gaussian03 program package [16]. The geometry optimization of **(I)** was converged at the threshold limits of 0.00045 and 0.0018 au were applied for the maximum force and displacement respectively. The topological analysis was carried out from the wave functions obtained from DFT theory. The bond topological properties such as electron density $\rho_{bcp}(r)$, Laplacian of electron density $\nabla^2\rho_{bcp}(r)$, eigen values ($\lambda_1, \lambda_2, \lambda_3$) and ellipticity ε were calculated from Bader's theory of Atoms in molecules (AIM) [17], which are implemented in AIMPAC program suite [18]. The deformation density of the molecule was plotted by *wfn2plots* and *Xdgraph* [19]. The MOLISO software [20] was used for the generation of ESP map of the molecule using the potential cube file of Gaussian03.

3. Results and discussion

3.1 Docking Studies

The lowest energy of 10 different conformers are presented in table 1. The nearest neighbours, shortest intermolecular contacts obtained from docking analysis are given in table 2. Figure 2 shows, some important intermolecular contact exist between dihydroxy coumarin and the cytochromeP450. Intermolecular interactions play an important role in the inhibition of an enzyme function. Various intermolecular forces such as hydrophobic, dispersion, van der Waals, hydrogen bonding and electrostatic are involved to form intermolecular association [21]. The Polar hydrogen atoms H(3) and H(4) present in the alcoholic group of dihyroxy coumarins forms more number of hydrogen bonding interactions with the cytochrome P450. The strongest hydrogen bonding interaction is exist between the oxygen atom of Ser119 and polar hydrogen atom H(4) at a distance of 1.9Å. The H(4) atom also makes another two strong hydrogen bonding interactions with the carbon atom of aminoacid residue Arg105 at 2.9 and 2.8Å respectively. The H···H interactions if formed between the NH_2 atom of Arg400 at a distance of 3.1Å. An electrostatic interaction is formed by the C(2) atom of coumarins molecule with oxygen atom of Ile120 at 2.7Å. The other atoms C(1), C(3), C(4), C(5), C(6), C(7), C(8), C(9), and all oxygen atoms present in the molecule forms hydrophobic interactions with Pro107, Arg105, Phe08, Ser119, Ile120 and Glu122, the corresponding interactions distances are presented in Table 2. Apart from these interactions, Dihydroxy coumarin forms hydrophobic and van der Waals interactions with the other nearest neighbours of aminoacid residue present in the active site of cytochromeP450.

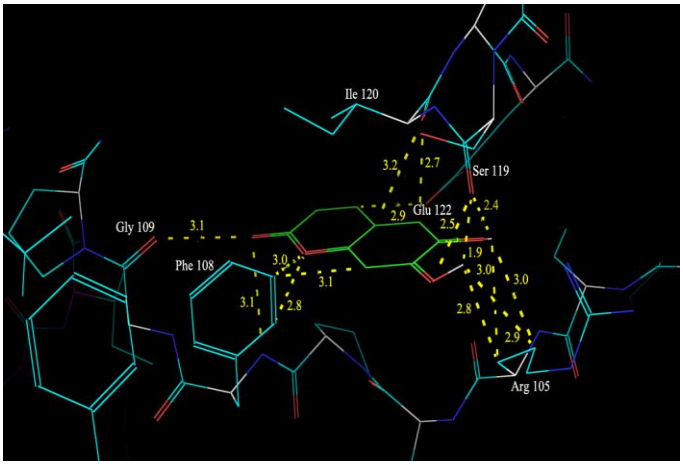

Figure 2. Coumarins-antigen85C complex showing some important intermolecular interactions in the active site of antigen85C.

3.2 Structural analysis

The conformation of the molecule was changed due to the intermolecular interactions that exist between the amino acid residues and the Coumarins molecule after it entering into the active site of cytochromeP450 [Figure.3]. As the bond length in the SPE is very low compare with B3LYP methods. Importantly, the conformational modification of two forms was determined from its geometrical parameters

Table 1: The lowest docked energies (kcal/mol) of 10 different conformers of Coumarins.

Conformation	Lowest docked energy (kcal/mol)
1	-7.59
2	-7.53
3	-7.41
4	-6.88
5	-6.65
6	-6.59
7	-6.57
8	-6.56
9	-6.27
10	-6.19

Table 2: Nearest neighbours and short contact distances (Å) of Coumarins with amino acid residues of cytochromeP450

active site ihyroxycoumarin⋯cytochromeP450	Distance	Dihyroxycoumarin⋯cytochromeP450	Distance
C(1)⋯Ile120/O	3.1	C(8)⋯Pro107/CB	3.4
Ser119/O	3.5	Pro107/CA	3.4
C(2)⋯Glu122/OE1	3.2	C(9)⋯Pro107/CA	3.2
Ile120/O	2.7	O(1)⋯Phe108/CD2	2.8
C(3)⋯Ile120/O	3.2	Phe108/CE2	3
Glu122/OE1	3.5	Phe108/N	3.1
C(4)⋯Ile120/CG2	3.4	Pro107/CA	3.3
Phe108/CD2	3.4	O(4)⋯Ser119/O	2.5
C(5)⋯Phe108/CE2	3.1	Arg105/CB	3
Phe108/CD2	3.1	Arg105/CD	3.4
C(6)⋯Ile120/CA	3.4	O(3)⋯Ser119/O	3.2
Ser119/O	3.2	Arg105/N	3.1
Arg105/CB	3.5	Arg105/CB	3.1
C(7)⋯Glu122/OE1	2.9	H(3)⋯Ser119/O	2.4
H(4)⋯Ser119/C	3.1	Ser119/C	3.5
Ser119/O	1.9	Arg105/CG	3
Arg105/NH1	3.4	Arg105/N	3.4
Arg105/CD	3.2	Arg400/NH2	3.1
Arg105/CG	2.9		
Arg105/CB	2.5		

[Table 3]. The conformational modification due to intermolecular interaction can be easily understood from the difference of the torsion angles between the two forms of molecule **(I)** and **(II)**. In gas phase Coumarins is a linear molecule, after entering into the active site, its structure changes into a more folded conformation. Notably, the conformation of the backbone bonds C(5)–C(4)–O(1)–C(9) changed from *trans* to *gauche*, it is evident from their torsion angles as the values in the gas phase and the active site are -149.6° to 180° respectively. The conformation of C(1)–C(2)–C(3)–C(4) bonds of **(I)** is -63.8° after entering into the active site the angle is -173.5°, confirms the conformation changes from g*auche* to *trans*. Similarly, the torsion angle of C(3)-C(4)-O(1)-C(9) and O(1)-C(4)-C(3)-C(7) are 29.8° and -179.4° respectively.

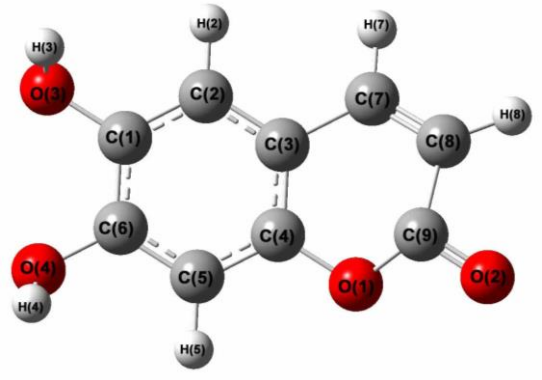

(a)

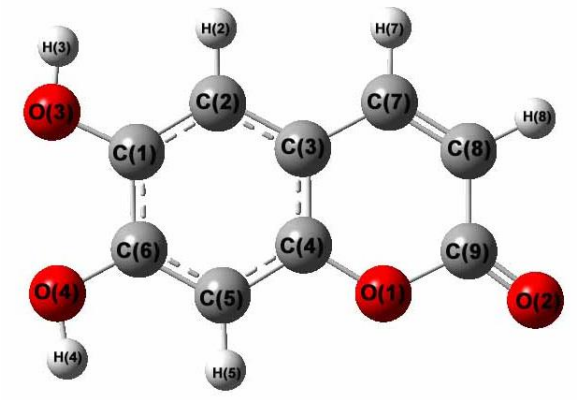

(b)

Figure.3 Optimized structure of Coumarins molecule (a) B3LYP/aug-cc-PVDZ and (b) Single point energy (SPE) calculation.

Table.3 Geometrical Parameters of Coumarins molecule

Bond length (Å)	SPE	B3LYP
C(1)–C(6)	1.386	1.418
C(1)–C(2)	1.386	1.381
C(1)–O(3)	1.410	1.363
C(6)–C(5)	1.386	1.388
C(6)–O(4)	1.410	1.356
C(5)–C(4)	1.386	1.394
C(5)–H(5)	1.122	1.084
C(4)–C(3)	1.386	1.401
C(4)–O(1)	1.410	1.362
C(3)–C(2)	1.386	1.410
C(3)–C(7)	1.540	1.435
C(2)–H(2)	1.122	1.086
O(1)–C(9)	1.410	1.403
C(9)–C(8)	1.548	1.455
C(9)–O(2)	1.213	1.201
C(8)–C(7)	1.324	1.352
C(8)–H(8)	1.122	1.081
C(7)–H(7)	1.122	1.086
O(3)–H(3)	0.992	0.963
O(4)–H(4)	0.992	0.963
Bond angle (°)		
C(6)–C(1)–C(2)	120	119.2
C(6)–C(1)–O(3)	120	116.5
C(2)–C(1)–O(3)	120	124.3
C(1)–C(6)–C(5)	120	120.1
C(1)–C(6)–O(4)	120	116.6
C(5)–C(6)–O(4)	120	123.3
C(6)–C(5)–C(4)	120	120
C(6)–C(5)–H(5)	120	121
C(4)–C(5)–H(5)	120	119
C(5)–C(4)–C(3)	120	120.9
C(5)–C(4)–O(1)	120	117.4
C(3)–C(4)–O(1)	120	121.7
C(4)–C(3)–C(2)	120	118.3
C(4)–C(3)–C(7)	120	117.3
C(2)–C(3)–C(7)	120	124.4
C(1)–C(2)–C(3)	120	121.5
C(1)–C(2)–H(2)	120	119.5
C(3)–C(2)–H(2)	120	119
C(4)–O(1)–C(9)	109.5	122.8
O(1)–C(9)–C(8)	120.9	115.5
O(1)–C(9)–O(2)	110.6	117.6
C(8)–C(9)–O(2)	110.6	126.8
C(9)–C(8)–C(7)	111.2	121.8
C(9)–C(8)–H(8)	124.2	115.5
C(7)–C(8)–H(8)	124.2	122.6
C(3)–C(7)–C(8)	120	120.9
C(3)–C(7)–H(7)	120	118.9
C(8)–C(7)–H(7)	120	120.2
C(1)–O(3)–H(3)	109.5	109.1
C(6)–O(4)–H(4)	109.5	109.3
Torsion angle (°)		
C(2)–C(1)–C(6)–C(5)	0	0
C(2)–C(1)–C(6)–O(4)	-179.4	180
O(3)–C(1)–C(6)–C(5)	-179.4	180
O(3)–C(1)–C(6)–O(4)	1.1	0
C(6)–C(1)–C(2)–C(3)	0	0
C(6)–C(1)–C(2)–H(2)	179.4	-180
O(3)–C(1)–C(2)–C(3)	179.4	-180
O(3)–C(1)–C(2)–H(2)	-1.1	0
C(6)–C(1)–O(3)–H(3)	120	180
C(2)–C(1)–O(3)–H(3)	-59.4	0
C(1)–C(6)–C(5)–C(4)	0	0
C(1)–C(6)–C(5)–H(5)	-179.4	-180
O(4)–C(6)–C(5)–C(4)	179.4	-180
O(4)–C(6)–C(5)–H(5)	0	0
C(1)–C(6)–O(4)–H(4)	-119	-180
C(5)–C(6)–O(4)–H(4)	60.6	0
C(6)–C(5)–C(4)–C(3)	0	0
C(6)–C(5)–C(4)–O(1)	179.4	180
H(5)–C(5)–C(4)–C(3)	179.4	-180
H(5)–C(5)–C(4)–O(1)	-1.1	0
C(5)–C(4)–C(3)–C(2)	0	0
C(5)–C(4)–C(3)–C(7)	-179.4	180
O(1)–C(4)–C(3)–C(2)	-179.4	180
O(1)–C(4)–C(3)–C(7)	1.1	0
C(5)–C(4)–O(1)–C(9)	-149.6	-180
C(3)–C(4)–O(1)–C(9)	29.8	0.1
C(4)–C(3)–C(2)–C(1)	0	0
C(4)–C(3)–C(2)–H(2)	-179.4	-180
C(7)–C(3)–C(2)–C(1)	179.4	-180

C(7)–C(3)–C(2)–H(2)	0	0
C(4)–C(3)–C(7)–C(8)	-16.1	0
C(4)–C(3)–C(7)–H(7)	163.3	180
C(2)–C(3)–C(7)–C(8)	164.5	-180
C(2)–C(3)–C(7)–H(7)	-16.1	0
C(4)–O(1)–C(9)–C(8)	-51.5	-0.1
C(4)–O(1)–C(9)–O(2)	176.8	-180
O(1)–C(9)–C(8)–C(7)	37.8	0
O(1)–C(9)–C(8)–H(8)	-135	-180
O(2)–C(9)–C(8)–C(7)	169.4	-180
O(2)–C(9)–C(8)–H(8)	-3.4	0
C(9)–C(8)–C(7)–C(3)	-2.2	0
C(9)–C(8)–C(7)–H(7)	178.4	-180
H(8)–C(8)–C(7)–C(3)	170.6	180
H(8)–C(8)–C(7)–H(7)	-8.8	0

4. Charge density analysis

The charge density analysis for the both forms [gas phase **(I)** and the same lifted from the active site **(II)**] was carried out. The cp search on all bonds invariably gave a (3, -1) type of critical point, which shows the existence of covalent bonds of the molecule [Figure.4]. The topological properties of the molecule are given in table 4.

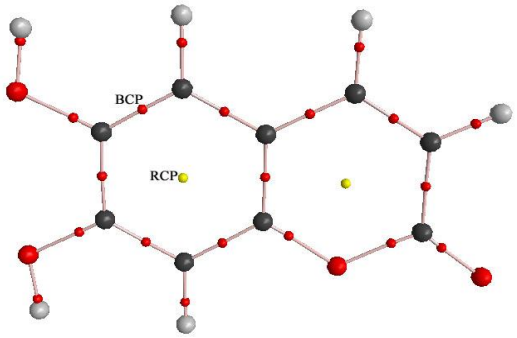

Figure 4 Theoretical molecular graph of the Coumarins molecule in gas phase. Black, blue, red and grey spheres show atomic positions. Small red and yellow spheres show bond (3,-1) and ring (3,+1) critical points in ρ, respectively.

Figure 5 (a,b) displays the deformation density map of (**I**) and **(II)** forms of Coumarins. As the molecule in the active site is highly twisted, the deformation density map of **(II)** significantly differs from **(I)**. The deformation density map clearly depicts the bonding regions and the lone pair positions of the molecule. The electron density of C–C

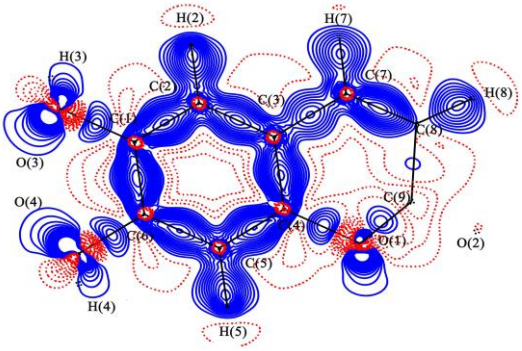

(a)

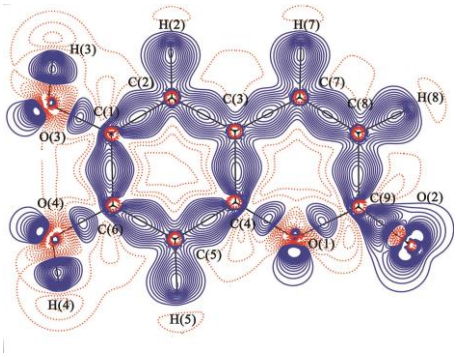

(b)

Figure 5: Deformation density maps of (a) **(I)** and (b) **(II)** forms of Coumarins molecule. Solid lines indicate positive contours, dotted lines are negative and dashed lines are zero contours. The contour interval is 0.05 eÅ^{-3}. [Since the molecule is highly twisted the electron density maps were drawn for different phases (fragments)].

bonds of gas phase molecule ranges from 1.721 to 2.162 eÅ^{-3}. Except for the C(3)–C(7) bond; the electron density of all other C–C bonds of active site molecule (II) increases and it is ranges from 1.938 to 0.053 eÅ^{-3}; whereas, for C(2)–C(3) bond, the $\rho_{bcp}(r)$ decreases from 1.628 to 1.602 eÅ^{-3}. The trend remains same in polar bonds in which the electron density of C(4)–O(1) and C(9)–O(1), bonds increases when the molecule present in the active site. The $\rho_{bcp}(r)$ of C(4)–O(1) and C(9)–O(2) of (I) is 1.789 and 1.748 eÅ^{-3} respectively, but the corresponding active site form of **II** are 1.751 and 1.969eÅ^{-3} respectively.

Table 4: Topological properties of electron density of Coumarins molecule calculated from DFT (SPE) and DFT methods. First line indicates SPE, second line indicates B3LYP/6-311G**.

Bonds	$\rho(r)^a$	$\nabla^2\rho^b$	ε	$\lambda_1{}^\beta$	$\lambda_2{}^\beta$	$\lambda_3{}^\beta$	$d_1{}^c$	$d_2{}^c$	D^c
C(1)–C(6)	2.162	-22.41	0.313	-17.243	-13.134	7.968	0.691	0.696	1.387
	2.053	-20.5	0.263	-16.118	-12.76	8.388	0.704	0.715	1.419
C(1)–C(2)	2.133	-21.64	0.261	-16.352	-12.962	7.68	0.679	0.708	1.386
	2.112	-21	0.278	-16.041	-12.548	7.581	0.666	0.722	1.388
C(1)–O(3)	2.125	-21.43	0.262	-16.229	-12.859	7.655	0.716	0.671	1.387
	2.097	-21	0.259	-16.017	-12.719	7.777	0.72	0.674	1.394
C(6)–C(5)	2.138	-21.69	0.266	-16.438	-12.987	7.735	0.68	0.707	1.386
	2.142	-21.5	0.296	-16.38	-12.635	7.545	0.667	0.714	1.381
C(6)–O(4)	2.138	-21.74	0.25	-16.357	-13.082	7.694	0.676	0.711	1.387
	2.087	-20.8	0.241	-15.893	-12.81	7.923	0.675	0.726	1.401
C(5)–C(4)	1.783	-13.19	0.044	-12.46	-11.931	11.202	0.502	0.909	1.411
	1.938	-9.7	0.037	-14.001	-13.506	17.785	0.467	0.897	1.364
C(5)–H(5)	2.111	-21.2	0.216	-15.828	-13.016	7.645	0.698	0.688	1.386
	2.008	-19.2	0.203	-14.797	-12.304	7.900	0.705	0.705	1.410
C(4)–C(3)	1.781	-12.14	0.032	-12.204	-11.828	11.894	0.914	0.496	1.410
	1.906	-6.9	0.012	-13.283	-13.124	19.509	0.901	0.462	1.363
C(4)–O(1)	1.789	-13.39	0.008	-12.522	-12.428	11.557	0.512	0.901	1.413
	1.751	-10.3	0.021	-12.112	-11.865	13.701	0.496	0.909	1.405
C(3)–C(2)	1.566	-11.88	0.112	-10.777	-9.688	8.586	0.745	0.808	1.553
	1.902	-17.9	0.15	-14.139	-12.296	8.509	0.701	0.755	1.456
C(3)–C(7)	2.803	-5.07	0.125	-27.274	-24.235	46.439	0.800	0.414	1.213
	2.864	-4.4	0.117	-27.554	-24.661	47.811	0.789	0.412	1.201
C(2)–H(2)	2.394	-26.52	0.33	-18.914	-14.224	6.616	0.652	0.672	1.324
	2.248	-23.5	0.286	-17.195	-13.373	7.088	0.664	0.688	1.352
O(1)–C(9)	1.593	-12.25	0.098	-10.865	-9.892	8.510	0.773	0.767	1.540
	1.940	-18.5	0.128	-14.154	-12.543	8.223	0.721	0.714	1.435
C(9)–C(8)	1.787	-13.54	0.05	-12.608	-12.009	11.075	0.503	0.908	1.411
	1.907	-23.6	0.006	-18.192	-18.074	12.695	0.373	0.698	1.071
C(9)–O(2)	1.748	-19.89	0.024	-16.202	-15.821	12.138	0.726	0.381	1.108
	1.969	-9.3	0.015	-14.316	-14.1	19.155	0.462	0.894	1.356
C(8)–C(7)	1.751	-19.95	0.023	-16.135	-15.773	11.960	0.385	0.723	1.108
	2.477	-61.1	0.021	-43.426	-42.523	24.812	0.767	0.173	0.940
C(8)–H(8)	1.750	-20.11	0.03	-16.503	-16.023	12.418	0.375	0.734	1.108
	1.882	-22.8	0.029	-17.846	-17.343	12.400	0.695	0.375	1.070
O(3)–H(3)	2.284	-51.53	0.03	-37.204	-36.128	21.803	0.193	0.778	0.971
	1.914	-23.6	0.027	-18.48	-17.992	12.869	0.369	0.698	1.066
O(4)–H(4)	2.281	-51.67	0.03	-37.257	-36.189	21.777	0.192	0.779	0.971
	2.482	-60.9	0.023	-43.327	-42.369	24.749	0.174	0.766	0.940

The $\rho_{bcp}(r)$ value of C–H bond of molecule ranges from 1.750 to 2.394 eÅ^{-3}. After, entering into the active site the electron density has been increased, the value ranges from 1.876 to 2.248 eÅ^{-3}. This shows that the charges of the C–H bond are become concentrated. The electron density of the polar O(3)–H(3) and O(4)–H(4) bonds density slightly increased from 2.281 to 2.284 eÅ^{-3} and 2.482 to 1.914 eÅ^{-3} respectively.

5. Laplacian of electron density

The Laplacian of electron density $\nabla^2\rho_{bcp}(r)$ of both forms of molecule **(I)** and **(II)** are listed in table 4. On comparing the Laplacian of electron density of both forms of the Coumarins, there are no substantial variation has been found in the C–C, C–O bonds of the molecule. The $\nabla^2\rho_{bcp}(r)$ of both forms of gas phase molecule **(I)** and docked form **(II)** are almost equal. The Laplacian of electron density of C–C bonds of molecule **(I)** and **(II)** ranges from -13.19 to -22.41 eÅ^{-5}, -6.9 to -21.0 eÅ^{-5} respectively. These values are almost close to the reported values. The average values of C–O bonds of molecule **(I)** and **(II)** are -12.2 eÅ^{-5} and -9.3 eÅ^{-5} respectively. The Laplacian of electron density of C–H [~ -26.2 eÅ^{-5}], O–H [~ -51.3 eÅ^{-5}] bonds in the active site are found to be slightly negative than the corresponding gas phase form of Coumarins **(I)**, indicates the bond charges become slightly concentrated when the molecule present in the active site

The dipole moment of the gas phase form of Coumarins molecule **(I)** is 4.43D, whereas this value has been found to be decreased in **(II)** and the value is 4.0D. The difference in dipole moment between the two forms is ~0.4D. This large enhancement of dipole moment is mainly due to the strong and weak intermolecular interactions that exist between the amino acid residues present in the active site of antigen85c and the Coumarins molecule. Table 5 displays the dipole moment values of Coumarins molecule in gas phase and in the active site.

Table. 5 Dipole moment of Coumarins molecule

Methods	X	Y	Z	Total
B3LYP/6-311G**	-3.4560	2.7762	0.0000	4.4330
SPE	-1.7434	2.6502	2.4367	4.0001

6 Electrostatic Potential

Figure 6 (a,b) shows the three-dimensional electrostatic potential map of Coumarins molecule (I) and (II). This clearly depicts the difference in electrostatic potential map of two forms [**(I)** & **(II)**] of Coumarins molecule and it insights the effect of intermolecular interactions.

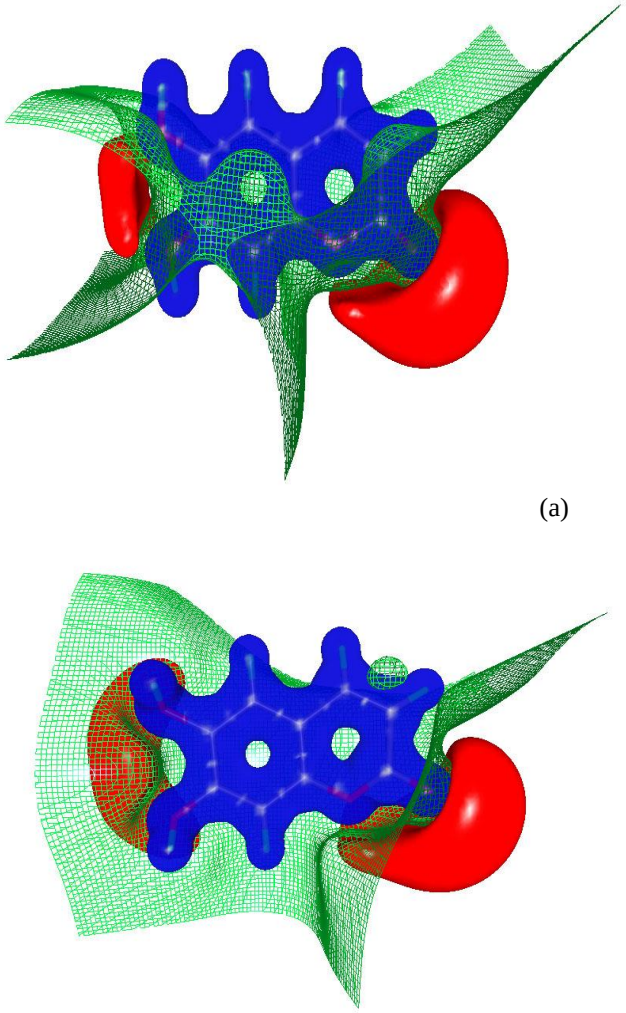

(a)

(b

Figure 6: Isosurface representation of molecular electrostatic potential of (a) **(I)** and (b) **(II)** forms of Coumarins molecule [B3LYP/6-311G**]. Blue: positive potential (+0.5 e/Å^{-1}) and Red: negative potential (-0.5 e/Å^{-1}). Green: Zero potential

A large electropositive region is found around the carbon atoms of molecule **(I)** and **(II)** and it acts as an electrophilic region and a large electronegative region is found at the vicinity of O(2), O(3) and O(4) atoms. These atoms act as a nucleophilic region and are forms hydrogen bonding and electrostatic interactions with the neighbouring amino acid groups. When compared to molecule **(I)** these regions are slightly extended in molecule **(II)** due to intermolecular interactions and charge redistribution.

7. Conclusions

The docking analysis of dihydroxycoumarins with cytochromeP450 was carried out. The charge density analysis also performed in gas phase molecule **(I)** and in the active site **(II)** to differentiate their topological and electrostatic properties. The molecule when it presents in the active site its conformation is changed into folded structure due to the intermolecular interactions and charge redistribution. The strongest hydrogen bonding interaction is exist between the oxygen atom of Ser119 and polar hydrogen atom H(4) at a distance of 1.9Å. Except for C(2)–C(3) bond, the electron density distribution of all other C–C bonds are increased when the molecule present in the active site. The oxygen atoms O(1), O(2) and O(3) are exhibiting high negative charge and are forming several intermolecular interactions with the amino acid residues in the active site of cytochromeP450. Due to the polarization and charge redistribution the dipole moment of the molecule of (**II**) is enhanced to 4.0D the corresponding value in gas phase is 4.43D. A large electronegative region is observed near the electronegative nitrogen and oxygen atoms and these atoms are act as a nucleophilic region.

Reference

1. Prakash D, Upadhyay G, Singh BN, Sing HB. Antioxidant and free radical-scavenging activities of seeds anda gri-wastes of some varieties of soybean (Glycine Max). Food Chem 2007; 104:783–790.
2. Hussain HH, Babic G, Durst T, Wright JS, Flueraru M, Chichirau A et al. Development of novel antioxidants: design, synthesis, and reactivity. J Org Chem 2003;68:7023–7032.
3. Siedle LG, Gustavsoon L, Johansson S, Murillo R, Castro V, Bohlin L, Merfot I. The effect of sesquiterpene lactones on the release of human neutrophil elastase. Biochem Pharmacol 2003; 65: 897–903.
4. Siedle B, Hrenn A, Merfort I. Natural compounds as inhibitors of human neutrophil elastase. Planta Med 2007;73:401–420.
5. Khlebnikov AI, Schepetkin IA, Quinn MT. Structure-activity relationship analysis of N-benzoylpyrazoles for elastase inhibitory activity: a simplified approach using atom pair descriptors. Bioorg Med Chem 2008;16:2791–2802.
6. K. N. Venugopala, V. Rashmi, and B. Odhav, Review on Natural Coumarin Lead Compounds for Their Pharmacological Activity, BioMed Research International, 2013. Volume 2013, Article ID 963248, 14 pages http://dx.doi.org/10.1155/2013/963248
7. Fylaktakidou, K.C., Hadjipavlou-Litina, D.J., Litinas, K.E.Nikolaides, "Natural and synthetic coumarin derivatives with anti-inflammatory/ antioxidant activities," Curr. Pharm. De.,10, 3813-3833, 2004
8. Manojkumar, P., Ravi, T.K., Gopalakrishnan, S., Eur. J. Med. Chem. 44, 4690–4694, 2009
9. Maria Joao Matos,a,* Lourdes Santana,a Patricia Janeiro,a Elías Quezada,a Eugenio Uriarte,a Humberto González-Díaz,b Dolores Viña,c and Francisco Oralloc , Design, Synthesis and Pharmacological Evaluation of New Coumarin Derivatives as Monoamine Oxidase A and B Inhibitors, 12th International Electronic conference on synthetic organic chemistry, 1-30 Nov. 2008.
10. Yano JK, Wester MR, Schoch GA, Griffin KJ, Stout CD, Johnson EF. J.Biol.Chem. 2004, 279, 38091.
11. G. M. Morris, R. S. Goodsell, R. S. Halliday, R. Huey, W. E. Hart, R. K. Belew and A. J. Olson, J. Comput. Chem., (1998), 19, 1639–1662.
12. W. L. DeLano. PyMol Molecular Graphics System, DeLano Scientific, San Carlos, CA, USA. (2002).
13. P. Politzer and J. S. Murray, Theo. Chem. Acc., (2002), 108, 134–142.
14. S. J. Smith and B. T. Sutcliffe. Rev. Comp. Chem. (1997), 10, 271–316
15. A. D. Becke, J. Chem. Phys. (1993), 98, 5648–5652.
16. M.J. Frisch, G.W. Trucks, H.B. Schlegel, G.E. Scuseria, M.A. Robb, J.R. Cheeseman, J.A. Montgomery, T. Vreven, K.N. Kudin, J.C. Burant, J.M Millam, S.S. Iyengar, J. Tomasi, V. Barone, B. Mennucci, M. Cossi, G. Scalmani, N. Rega, G.A. Petersson, H. Nakatsuji, M. Hada, M. Ehara, K. Toyota, R. Fukuda, J. Hasegawa, M. Ishida, T. Nakajima, Y. Honda, O. Kitao, H. Nakai, M. Klene, X. Li, J.E. Knox, H.P. Hratchian, J.B. Cross, C. Adamo, J. Jaramillo, R. Gomperts, R.E. Stratmann, O. Yazyev, A.J. Austin, R. Cammi, C. Pomelli, J.W. Ochterski, P.Y. Ayala, Morokuma, G.A. Voth, P. Salvador, J.J. Dannenberg, V.G. Zakrzewski, S. Dapprich, A.D. Daniels, M.C. Strain, O. Farkas, D.K. Malick, A.D. Rabuck, K. Raghavachari, J. B. Foresman, J.V. Ortiz, Q. Cui, A.G. Baboul, S. Clifford, J. Cioslowski, B.B. Stefanov, G. Liu, A. Liashenko, P. Piskorz, I. Komaromi, R.L. Martin, D.J. Fox, T. Keith, M.A. Al-Laham, C.Y. Peng, A. Nanayakkara, M. Challacombe, P.M.W. Gill, B. Johnson, W. Chen, M.W. Wong, C. Gonzalez and J.A. Pople. Gaussian03, Revision D.1; Gaussian, Inc., Wallingford, CT, (2005).
17. R.F.W.Bader, Y. Tal, S.G. Anderson & T.T. Nguyen-Dang. Isr. J. Chem. (1980), 19, 8–29.
18. J. Cheeseman, T.A. Keith & R.F.W. Bader. AIMPAC Program Package,McMaster University Hamilton, Ontario. (1992).
19. T. Koritsanszky, P. Macchi, C. Gatti, L.J. Farrugia, P.R. Mallinson, A. Volkov and T. Richter. XD-2006. A Computer Program Package for Multipole Refinement and Topological Analysis of Charge Densities and Evaluation of Intermolecular Energies from Experimental or Theoretical Structure Factors, Version 5.33, (2007).
20. C.B. Hubschle and P. Luger. J. Appl. Crystallogr. (2006), 39, 901–904.
21. Rama Rao Nadendla, Resonance, (2004), 51–60.